Geometry tolerance estimation for rectangular dielectric waveguide devices by means of perturbation theory

Manfred Lohmeyer, Norbert Bahlmann, Peter Hertel
Department of Physics, University of Osnabrück,
Barbarastraße 7, D-49069 Osnabrück, Germany

Abstract: Alteration of a geometry parameter in the cross section of a dielectric waveguide with piecewise constant permittivity profile can be regarded as a refractive index perturbation in a layer along a dielectric discontinuity line. Starting from these thin layer perturbations, we derive explicit expressions for partial derivatives of propagation constants with respect to the transverse waveguide dimensions, both for hybrid modes and for fields calculated in the semivectorial approximation. The perturbational formulas allow to estimate fabrication tolerances for realistic integrated optics devices at almost no extra computational cost. We demonstrate this by the example of a simple directional coupler and compare the perturbational results to numerically calculated tolerances.

Keywords: integrated optics, dielectric waveguides, guided modes, numerical modeling, fabrication tolerances
PACS codes: 42.82.–m 42.82.Et

1 Introduction

A variety of integrated optical devices is based on the interference of modes propagating along longitudinally homogeneous waveguide sections. If a dimensional parameter in the guiding structure is slightly altered, in first order only the mode wavenumbers change, while the amplitude coefficients are almost unaffected. It is therefore a good approximation to consider only the propagation constant alteration to estimate the deviation of the power transmission.

For this purpose, expressions for the gradients of mode propagation constants with respect to the variation of geometry dimensions would be helpful. In a waveguide with piecewise constant refractive index profile, e.g. enlargement of a layer thickness can be regarded as changing the permittivity within a thin slice on top of the layer. While expressions for the wavenumber shift due to such thin layer perturbations are known but seemingly rarely applied [1], we investigate in this paper their interpretation as geometry modifications. An example of an analogous treatment for the scalar modes of weakly guiding circular step index fibers can be found in [2].

Following the reasoning of [1], in Sec. 2 the thin layer formulas are applied to derive wavenumber gradients due to the movement of boundaries between regions of different permittivity. Sec. 3.1 provides numerical verification of these expressions for a series of simple raised strip waveguides. In Sec. 3.2 we show that the formulas can be successfully applied to estimate the fabrication tolerances for a directional coupler based on these waveguides.

2 Perturbational expressions for geometry variations

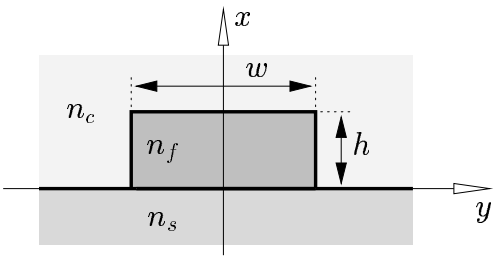

Figure 1: A simple waveguide: the cross section plane may be divided into rectangles with uniform refractive index, discontinuity lines are parallel to the cross section coordinate axes.

Fig. 1 shows the cross section of a raised strip waveguide, an example for the lossless rectangular structures with piecewise constant isotropic permittivity $\epsilon = n^2$ investigated in this paper. Denote by x and y the transverse

coordinates normal and parallel to the substrate surface and by z the direction of propagation. Assuming a dependence $\sim \exp(\mathrm{i}\omega t - \mathrm{i}\beta z)$ in time and on the propagation distance, the electric $\boldsymbol{E}(x,y)$ and magnetic fields $\boldsymbol{H}(x,y)$ corresponding to a usually hybrid guided mode with propagation constant β are governed by Maxwell's curl equations

$$(\mathrm{C} + \mathrm{i}\beta\mathrm{R})\boldsymbol{E} = -\mathrm{i}\omega\mu_0\boldsymbol{H}, \quad (\mathrm{C} + \mathrm{i}\beta\mathrm{R})\boldsymbol{H} = \mathrm{i}\omega\epsilon_0\epsilon\boldsymbol{E}, \tag{1}$$

with C and R defined as

$$\mathrm{C} = \begin{pmatrix} 0 & 0 & \partial_y \\ 0 & 0 & -\partial_x \\ -\partial_y & \partial_x & 0 \end{pmatrix} \quad \text{and} \quad \mathrm{R} = \begin{pmatrix} 0 & 1 & 0 \\ -1 & 0 & 0 \\ 0 & 0 & 0 \end{pmatrix}. \tag{2}$$

μ_0 and ϵ_0 are the vacuum permeability and permittivity, the frequency ω is connected with the vacuum wavelength λ and wavenumber k by $\omega\sqrt{\epsilon_0\mu_0} = k = 2\pi/\lambda$.

Using the scalar product notation $(\boldsymbol{F}, \boldsymbol{G}) = \iint \boldsymbol{F}^*\boldsymbol{G}\,\mathrm{d}x\,\mathrm{d}y$, the following form can be defined [1] as a functional of the six separate fields $E_x, \ldots, H_z$:

$$\mathrm{B}_\epsilon(\boldsymbol{E}, \boldsymbol{H}) = \frac{\omega\epsilon_0(\boldsymbol{E}, \epsilon\boldsymbol{E}) + \omega\mu_0(\boldsymbol{H}, \boldsymbol{H}) + \mathrm{i}(\boldsymbol{E}, \mathrm{C}\boldsymbol{H}) - \mathrm{i}(\boldsymbol{H}, \mathrm{C}\boldsymbol{E})}{(\boldsymbol{E}, \mathrm{R}\,\boldsymbol{H}) - (\boldsymbol{H}, \mathrm{R}\,\boldsymbol{E})}. \tag{3}$$

B_ϵ is stationary at a valid mode field, i.e. for $\boldsymbol{E}$ and $\boldsymbol{H}$ satisfying Eqs. (1); it then evaluates to the propagation constant $\beta = \mathrm{B}_\epsilon(\boldsymbol{E}, \boldsymbol{H})$.

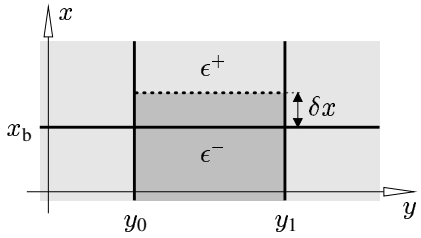

Figure 2: Horizontal boundary variation: For $y_0 < y < y_1$, the boundary at $x = x_\mathrm{b}$ separating permittivities ϵ^- below and ϵ^+ above is shifted by a small distance δx.

Now we suppose the propagation constant β and field $\boldsymbol{E}$, $\boldsymbol{H}$ corresponding to the permittivity profile ϵ to be known, and consider the variation of a dimensional parameter in the waveguide geometry as sketched in Fig. 2. Shifting the horizontal boundary changes the permittivity to $\epsilon + \delta\epsilon$, with

$$\delta\epsilon\,(x,y) = \begin{cases} (\epsilon^- - \epsilon^+) & \text{for } x_\mathrm{b} < x < x_\mathrm{b} + \delta x,\ y_0 < y < y_1, \\ 0 & \text{otherwise.} \end{cases} \tag{4}$$

Along with the permittivity, both the propagation constant and the field will change by small amounts $\delta\beta$, $\delta\boldsymbol{E}$, $\delta\boldsymbol{H}$, where the modified quantities are connected by the functional $\mathrm{B}_{\epsilon+\delta\epsilon}$:

$$\beta + \delta\beta = \mathrm{B}_{\epsilon+\delta\epsilon}(\boldsymbol{E} + \delta\boldsymbol{E}, \boldsymbol{H} + \delta\boldsymbol{H}). \tag{5}$$

We are interested in a good estimate for the change $\delta\beta$ of the propagation constant. Since B_ϵ is stationary at $\boldsymbol{E}$, $\boldsymbol{H}$, inserting plausible expressions for the modified fields should be sufficient.

The small boundary shift will not significantly affect the overall mode shape. At a boundary parallel to the y-z plane, E_y, E_z, H_x, H_y, and H_z are continuous, therefore the original profiles should be good approximations to the modified fields for these components. In contrast, E_x jumps due to the continuity of the dielectric displacement: $\epsilon^- E_x^- = \epsilon^+ E_x^+$, where field superscripts $+, -$ denote appropriate limits on the horizontal boundary line. With the location of the boundary, the jump shifts from $x = x_\mathrm{b}$ to $x_\mathrm{b} + \delta x$, while $E_x + \delta E_x$ must be continuous in x_b. This is illustrated in Fig. 3.

For the modified geometry, the continuity requirements are satisfied in zeroth order, if one chooses $\delta\boldsymbol{H} = 0$, $\delta E_y = \delta E_z = 0$, and

$$\delta E_x(x,y) = \begin{cases} \dfrac{(\epsilon^+ - \epsilon^-)}{\epsilon^-} E_x(x,y) & \text{for } x_\mathrm{b} < x < x_\mathrm{b} + \delta x,\ y_0 < y < y_1, \\ 0 & \text{otherwise.} \end{cases} \tag{6}$$

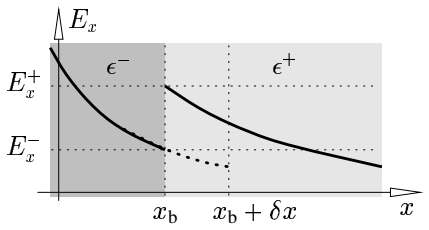

Figure 3: Boundary shift from x_b to $x_\mathrm{b}+\delta x$. E_x changes from the continuous to the dotted curve.

Insertion of these expressions into Eq. (5) and neglection of terms $\sim \delta\beta\,\delta\boldsymbol{E}$ yields, with help of Eqs. (1):

$$\delta\beta = \omega\epsilon_0 \frac{(\delta\boldsymbol{E}, \epsilon\,\delta\boldsymbol{E}) + (\boldsymbol{E}+\delta\boldsymbol{E}, \delta\epsilon\,(\boldsymbol{E}+\delta\boldsymbol{E}))}{(\boldsymbol{E}, \mathrm{R}\,\boldsymbol{H}) - (\boldsymbol{H}, \mathrm{R}\,\boldsymbol{E})}\,. \tag{7}$$

Using Eqs. (4,6), this transforms to an expression for the propagation constant change due to a thin layer perturbation [1]:

$$\delta\beta = \frac{\omega\epsilon_0}{2} \frac{(\epsilon^- - \epsilon^+) \iint_\square \left(\frac{\epsilon^+}{\epsilon^-}|E_x|^2 + |E_y|^2 + |E_z|^2\right) \mathrm{d}x\,\mathrm{d}y}{\iint \left(E_x H_y^* - E_y H_x^*\right) \mathrm{d}x\,\mathrm{d}y}\,. \tag{8}$$

Here $\square$ indicates the rectangle $x_\mathrm{b} < x < x_\mathrm{b}+\delta x,\ y_0 < y < y_1$.

For a small shift, the fields do not change significantly along x on $\square$, thus the x integration in the numerator can be skipped, leading to the desired estimate for the derivative of the propagation constant with respect to the boundary location:

$$\delta\beta = \frac{\omega\epsilon_0}{2} \frac{(\epsilon^- - \epsilon^+) \int_{y_0}^{y_1} \left((E_x^+)^* E_x^- + |E_y|^2 + |E_z|^2\right)(x_\mathrm{b}, y)\,\mathrm{d}y}{\iint \left(E_x H_y^* - E_y H_x^*\right) \mathrm{d}x\,\mathrm{d}y}\,\delta x\,. \tag{9}$$

As it should be, the propagation constant is influenced by a geometry dimension only if the boundary separates regions made of different materials and if the mode field is not negligible on the relevant line. Note that the first term in the numerator can alternatively be written $(E_x^+)^* E_x^- = \epsilon^+ |E_x^+|^2/\epsilon^- = \epsilon^- |E_x^-|^2/\epsilon^+ = |\epsilon E_x|^2/(\epsilon^-\epsilon^+)$. There are no ambiguities regarding the discontinuity of E_x on the boundary. In fact, Eq. (9) can be arrived at if one considers moving the boundary line in the negative x-direction (cf. Fig. 2) and rewrites expressions (4,6) accordingly.

Exchanging the role of x and y yields the corresponding formula for the variation of a vertical discontinuity line. Consider the boundary $y = y_\mathrm{b}$, $x_0 < x < x_1$ separating permittivities ϵ^- on the left ($y < y_\mathrm{b}$) and ϵ^+ on the right ($y > y_\mathrm{b}$). Then the propagation constant changes by

$$\delta\beta = \frac{\omega\epsilon_0}{2} \frac{(\epsilon^- - \epsilon^+) \int_{x_0}^{x_1} \left(|E_x|^2 + (E_y^+)^* E_y^- + |E_z|^2\right)(x, y_\mathrm{b})\,\mathrm{d}x}{\iint \left(E_x H_y^* - E_y H_x^*\right) \mathrm{d}x\,\mathrm{d}y}\,\delta y\,, \tag{10}$$

if the boundary is shifted to $y = y_\mathrm{b} + \delta y$.

Frequently waveguide analysis is restricted to the so-called semi-vectorial approximation [3]. In case of TE polarized modes, only the dominant transverse electric component E_y is considered, with E_x assumed to vanish. For our piecewise constant profiles, a quasi-TE mode is defined as a field E_y satisfying the wave equation $(\partial_x^2 + \partial_y^2 + k^2\epsilon - \beta^2)E_y = 0$ inside the homogeneous rectangles, with continuous fields E_y, $\partial_x E_y$ on horizontal boundaries and ϵE_y, $\partial_y E_y$ on vertical boundaries. Likewise for TM polarized modes, H_x is assumed to vanish. The dominant magnetic component H_y must satisfy the wave equation everywhere but on the boundaries, where H_y and $\epsilon^{-1}\partial_x H_y$ are continuous for a horizontal line, and with continuous H_y and $\partial_y H_y$ on vertical lines.

Inserting this approximation into Eq. (9,10) yields the following expressions for the propagation constant shift of a quasi TE mode due to the movement of a horizontal boundary,

$$\delta\beta = \frac{k_0^2}{2\beta} \frac{(\epsilon^- - \epsilon^+) \int_{y_0}^{y_1} \left(|E_y|^2 + \beta^{-2} |\partial_y E_y|^2 \right) (x_\mathrm{b}, y)\, \mathrm{d}y}{\iint \left(|E_y|^2 - \beta^{-2} E_y \partial_y^2 E_y^* \right) \mathrm{d}x\, \mathrm{d}y} \delta x\,, \tag{11}$$

and

$$\delta\beta = \frac{k_0^2}{2\beta} \frac{(\epsilon^- - \epsilon^+) \int_{x_0}^{x_1} \left((E_y^+)^* E_y^- + \beta^{-2} |\partial_y E_y|^2 \right) (x, y_\mathrm{b})\, \mathrm{d}x}{\iint \left(|E_y|^2 - \beta^{-2} E_y \partial_y^2 E_y^* \right) \mathrm{d}x\, \mathrm{d}y} \delta y \tag{12}$$

for the movement of a vertical boundary. If one accepts the approximation of a negligible derivative $\beta^{-1}\partial_y E_y$ along a horizontal discontinuity, Eq. (11) can be simplified to

$$\delta\beta = \frac{k_0^2}{2\beta} \frac{(\epsilon^- - \epsilon^+) \int_{y_0}^{y_1} |E_y|^2 (x_\mathrm{b}, y)\, \mathrm{d}y}{\iint |E_y|^2 \mathrm{d}x\, \mathrm{d}y} \delta x\,. \tag{13}$$

For an alteration of the rib height of the waveguides considered in Sec. 3.1, we have found this approximation to be adequate. At the same time the corresponding simplification of Eq. (12) yields no acceptable results for the variation of the rib width, since the maxima of the longitudinal electric component $E_z = -\mathrm{i}\beta^{-1}\partial_y E_y$ are located on the rib flanks, thus the contributions are not negligible.

In case of quasi TM modes the electric fields are to be expressed by the magnetic component H_y. Now the expression for the wavenumber shift caused by moving a horizontal boundary reads

$$\delta\beta = \frac{\beta}{2} \frac{(\epsilon^- - \epsilon^+) \int_{y_0}^{y_1} \left(\frac{1}{\epsilon^- \epsilon^+} |H_y - \beta^{-2} \partial_y^2 H_y|^2 + \beta^{-4} |\partial_y \frac{1}{\epsilon} \partial_x H_y|^2 + \beta^{-2} |\frac{1}{\epsilon} \partial_x H_y|^2 \right) (x_\mathrm{b}, y)\, \mathrm{d}y}{\iint \frac{1}{\epsilon} \left(H_y - \beta^{-2} \partial_y^2 H_y \right) H_y^*\, \mathrm{d}x\, \mathrm{d}y} \delta x\,. \tag{14}$$

As in the TE case, the derivatives ∂_y can be dropped in Eq. (14) without noticeably affecting the results given in Sec. 3.1. Note that the terms $\sim 1/\epsilon$ in the numerator may be evaluated alternatively as $(\partial_x H_y)^+/\epsilon^+$ or $(\partial_x H_y)^-/\epsilon^-$.

While quasi TM modes satisfy the continuity requirements for H_y and H_z on vertical boundaries exactly, the conditions for the electric field components are significantly violated. Therefore Eq. (10) can hardly be expected to give satisfying results if quasi TM mode fields are inserted. A way out is the observation, that the TM boundary conditions on a vertical discontinuity are identical to the TE conditions on a horizontal line, while inside the homogeneous regions the same wave equation holds. Thus a promising candidate for the TM propagation constant shift due to a vertical boundary variation should be Eq. (13), with E_y substituted by H_y and x and y exchanged:

$$\delta\beta = \frac{k_0^2}{2\beta} \frac{(\epsilon^- - \epsilon^+) \int_{x_0}^{x_1} |H_y|^2 (x, y_\mathrm{b})\, \mathrm{d}x}{\iint |H_y|^2 \mathrm{d}x\, \mathrm{d}y} \delta y\,. \tag{15}$$

Maybe in an alternative way this or a modified equation can be rigorously derived. However, in our simulations we have found it to be correct up to the same accuracy as the expressions for TE and hybrid modes. The problem does not arise with quasi TE modes. For the component E_y entering the numerator of Eq. (12), the correct continuity requirements on vertical boundaries are enforced by definition.

3 Numerical results

For the waveguides investigated in this section we assumed parameters typical for magnetooptic garnet materials [4]. The refractive index values are such that the structures can neither be regarded weakly guiding, nor are the fields at the waveguide/air interfaces almost vanishing. Effects due to the jumps of the mode fields and derivatives at the dielectric discontinuities can thus be expected to be large, providing a good test for the perturbation formulas.

The mode fields and propagation constants are computed with the semivectorial and fully vectorial versions of a recently proposed mode solver [5, 6]. It is based on plane wave expansions, separately for regions with constant repfractive index. The semianalytical modal fields take into account the continuity requirements at dielectric interfaces explicitely and allow for a convenient evaluation of line- and surface integrals.

3.1 Raised Strip Waveguides

Besides the wavelength and the refractive indices, two geometry parameters define the waveguide sketched in Fig. 1: the rib height h and width w. Changing these dimensions can be interpreted as moving the enclosing boundaries. Thus first order effects on the propagation constants, i.e. the gradients in the curves $\beta(h)$, $\beta(w)$, are given by the perturbation expressions of the preceding section. For a verification we have calculated the dispersion curves, inserting secants with gradients as predicted by formulas (9, 10, 11, 12, 14, 15) for a few abscissas. Ideally these secants should be tangents at the evaluation points, and this is almost the case as shown in Fig. 4 for hybrid mode fields and in Fig. 5 for fields calculated with the semivectorial approximation.

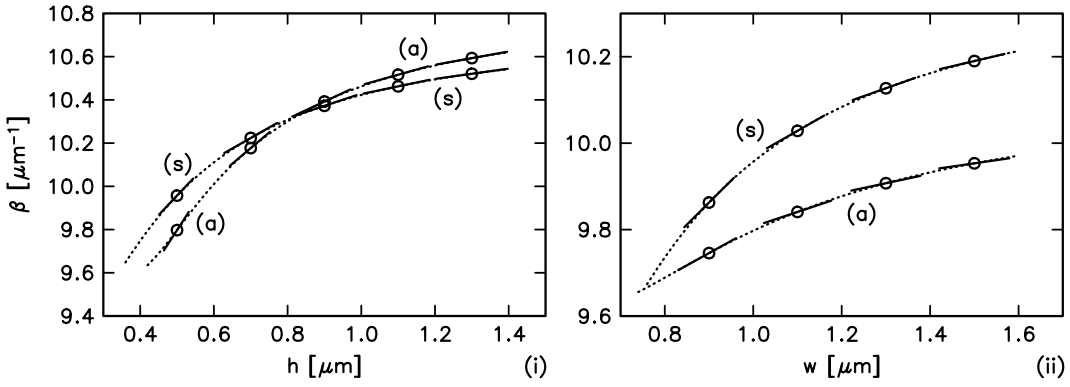

Figure 4: Dependence of the hybrid mode propagation constants β on the height h (i) and on the width w (ii) of a raised strip waveguide as sketched in Fig. 1, for symmetric (s) and antisymmetric (a) trial fields (see the text). The dotted lines correspond to multiple runs of the mode solver for varied parameters, while the continous sections show the tangents predicted by the evaluation of Eqs. (9,10), at the points indicated by circles. Parameters are $n_s = 1.95$, $n_f = 2.3$, $n_c = 1.0$, $\lambda = 1.3\,\mu$m, $w = 1.0\,\mu$m (i), and $h = 0.5\,\mu$m (ii).

In the calculations for Fig. 4, explicitely imposed modal symmetry with respect to $y = 0$ was used to separate the fundamental hybrid modes of different polarization. Trial fields with even components H_x, E_y, H_z and odd H_y, E_x, E_z (denoted (s) in Fig. 4) resulted in TE-dominant modes, those with reversed symmetry in TM-dominant modes. Due to opposite symmetry, the two $\beta(h)$-curves do not repel each other. No strong hybridization occurs for the degenerate modes around $h = 0.8\,\mu$m where the two curves cross.

Usually the way of applying the perturbation formulas is not unambiguous. Enlargement of the rib width can be simulated by evaluating Eq. (10, 12, 15) on the right or on the left sidewall (with a negative sign), or as an average of both. Likewise, to investigate an extended rib height, the perturbation formulas for horizontal boundary variation may be applied to the top surface or alternatively to the three sections of the rib baseline, with the results added. While the values for the gradient $\partial_w\beta$ are exactly equal due to the modal symmetry, agreement of the values for $\partial_h\beta$ estimated in both ways is not a priory obvious. We have carried out this test by recalculating $\partial_h\beta$ for semivectorial and hybrid fields and found no change with respect to Figs. (4,5).

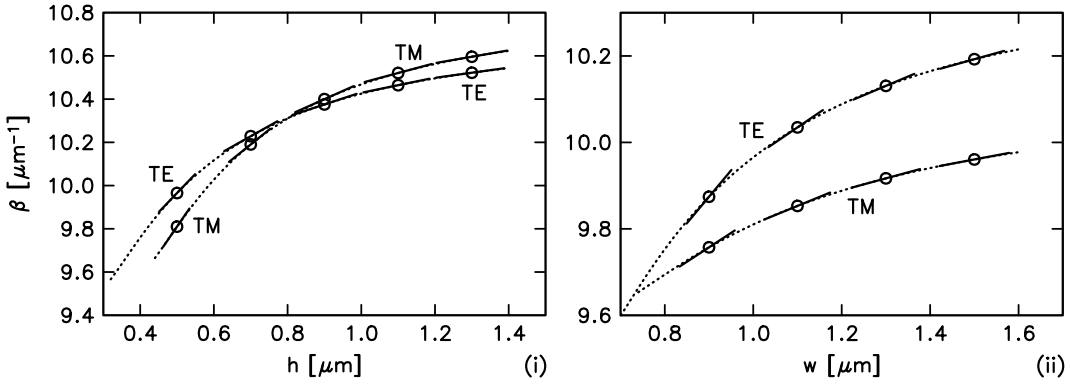

Figure 5: Analogon to Fig. 4, but for the fundamental semivectorial modes of both polarizations with Eqs. (11,12, 14,15) applied. Symbols and parameters are as given in the caption of Fig. 4.

3.2 Two-Waveguide Coupler

Two parallel waveguides at a small distance form the central part of a directional coupler. Fig. 6 illustrates mode shapes in a device made up from the waveguides of the previous section. Power transfer between them is determined by the interference of the supermodes.

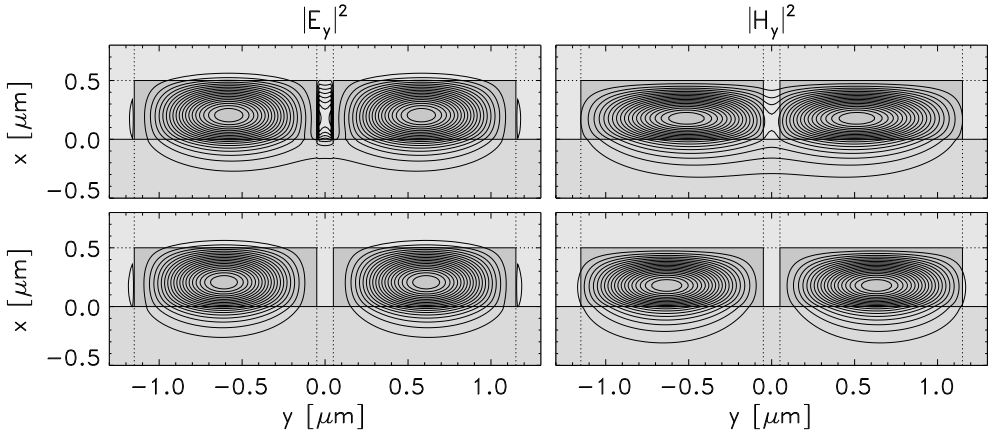

Figure 6: Intensity profiles for the symmetric (top) and antisymmetric (bottom) TE- (left) and TM-polarized (right) modes of a directional coupler made of two identical waveguides as sketched in Fig. 1. Waveguide dimensions are the height and width of the ribs $h = 0.5\,\mu$m, $w = 1.1\,\mu$m, and the spacing $g = 0.1\,\mu$m in-between, with other parameters as given for Fig. 4. The corresponding propagation constants are $10.0505\,\mu m^{-1}$ (TE, symm.), $10.0121\,\mu m^{-1}$ (TE, antis.), $9.9021\,\mu m^{-1}$ (TM, symm.), $9.8095\,\mu m^{-1}$ (TM, antis.).

For fixed polarization, denote by ϕ_l, ϕ_r the single modes of the left and right isolated waveguides and by ψ_s, ψ_a the symmetric and antisymmetric supermode of the entire structure. Suppose the coupling section to be excited by the mode of the left waveguide ϕ_l, with unit power input. Neglecting reflections, the relative power coupled out to the mode of the opposite waveguide ϕ_r after propagating along the devicelength L is then given by

$$P(L) = w_\mathrm{s}^2 + w_\mathrm{a}^2 + 2w_\mathrm{s}w_\mathrm{a}\cos((\beta_\mathrm{s} - \beta_\mathrm{a})L) \tag{16}$$

where the factors w_s, w_a are defined by the mode overlaps at input and output: $w_\mathrm{j} = \langle \phi_\mathrm{r}, \psi_\mathrm{j} \rangle \, \langle \psi_\mathrm{j}, \phi_\mathrm{l} \rangle$, $j =$ s,a. $\langle \, . \, , \, . \, \rangle$ is a bilinear product suitable to express supermode orthogonality. All modes involved are meant to be normalized with respect to this product. Without loss of generality, real weights $w_\mathrm{s}w_\mathrm{a} < 0$ were assumed.

According to Eq. (16), in devices of length $L = L_\mathrm{c} = \pi/(\beta_s - \beta_a)$ or $L = L_\mathrm{c}/2$ power is completely transferred to the right waveguide or equally distributed between the two waveguides, respectively. In our example, stronger coupling for TM fields resulted in a shorter coupling length (see the caption of Fig. 7) and a larger mismatch between the supermodes of Fig. 6 and the outer waveguide modes. The latter shows up in the

maximum power transmission through the untapered structures of $P(L_c) = 0.999$ for TE and $P(L_c) = 0.982$ for TM polarization.

If a dimensional parameter in the coupling region is altered, in first order perturbation theory only the propagation constants of the supermodes change, while the mode fields and thus their weights in the power transfer expression (16) are not affected. The main contribution to the change in the power troughput will be due to the altered supermode wavenumbers, to which the perturbation formulas of Sec. 2 give direct access. For a verification, Fig. 7 compares the relative output power $P(L_c)$, $P(L_c/2)$ from repeated mode calculations for the modified geometries to perturbational results. These were obtained in the following way. With fields from only one mode analysis for the original geometry the gradients of the supermode propagation constants $\partial_q \beta_s$, $\partial_q \beta_a$ corresponding to the change of one parameter $q = g, w, h$ are computed. Note that usually the formulas (11, 12, 14, 15) must be applied more than once at different boundaries, with the results added or subtracted. Power transmission through the device with dimension $q + \delta q$ is then approximated by Eq. (16), with fixed weights, but with the propagation constants replaced by $\beta_{s,a} + \partial_q \beta_{s,a} \delta q$.

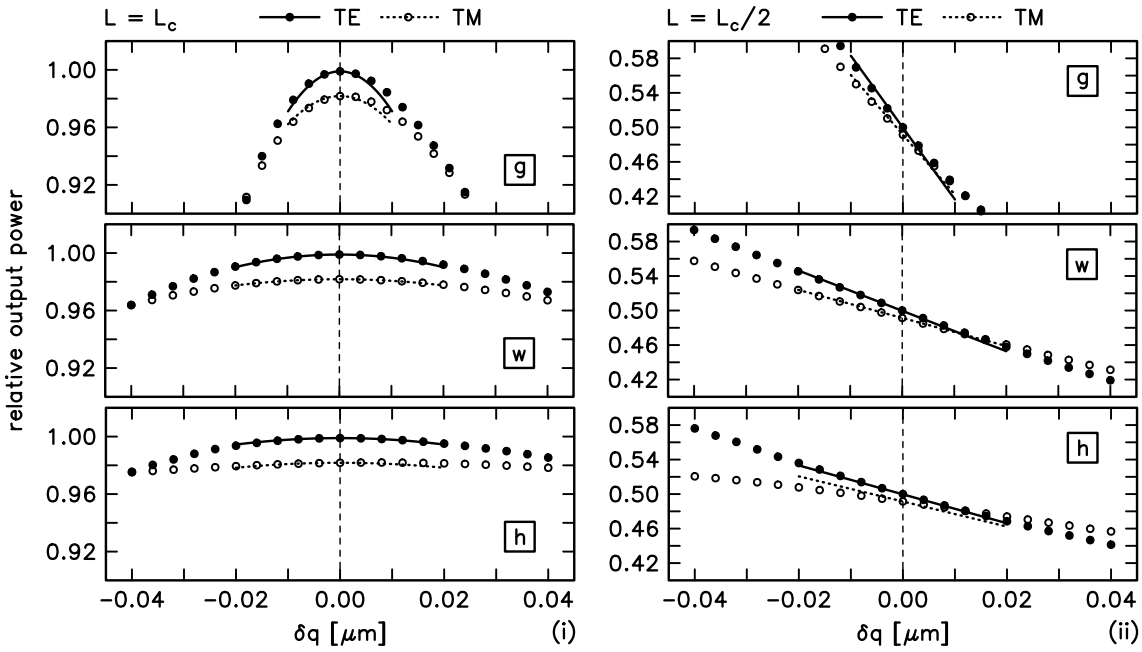

Figure 7: Dependence of the relative output power on geometry parameter variations for a directional coupler corresponding to Fig. 6. Modified parameters are the spacing g (top), the width w (center), and the height h (bottom) of the ribs. Only one parameter $q = g, w, h$ is altered to $q + \delta q$, with q and the remaining dimensions as given for Fig. 6. Markers correspond to complete semivectorial analysis runs with recalculation of the mode fields for the modified geometry, while the lines show the results of evaluating Eq. (16) and the perturbation formulas (11, 12, 14, 15) for the original parameter sets. The device length L was set to L_c (i) and $L_c/2$ (ii), with $L_c = 81.8\ \mu$m for TE polarization (filled circles, continuous lines) and $L_c = 33.9\ \mu$m for TM polarization (open circles, dotted lines).

Via β_s, β_a, P can be regarded a function of the three geometry parameters $q = g, w, h$. Assuming unaltered weights $|w_s| = |w_a| = 1/2$, expanding P with respect to one of these parameters q yields expressions for admissible geometry tolerances Δq for a given maximum deviation ΔP of the transmitted power. Evaluated at $L = L_c$, this reads

$$\Delta q = \pm \frac{2\sqrt{\Delta P}}{L\,|\partial_q \beta_s - \partial_q \beta_a|}, \tag{17}$$

and for $L = L_c/2$, one obtains

$$\Delta q = \pm \frac{2\Delta P}{L\,|\partial_q \beta_s - \partial_q \beta_a|}. \tag{18}$$

These expressions should be read as follows. Parameter values from $[q - \Delta q, q + \Delta q]$ allow for transmissions

above $P - \Delta P$ ($L = L_c$) or between $P - \Delta P$ and $P + \Delta P$ ($L = L_c/2$), respectively, if P is the power output for the original dimension q. Of course, similar formulas can be written for other input/output configurations.

For a more quantitative assessment, in the top part Table 1 compares propagation constant gradients from perturbation theory with those obtained by finite difference evaluation of mode analysis results. In the bottom half, the table contrasts geometry tolerances as can be read from the charts of Fig. 7 with the simple perturbational values according to Eqs. (17, 18). There is a good overall agreement, with the largest deviation occurring for the rib height variation in TM polarization. Although the gradients entering Eqs. (17, 18) are evaluated with a small relative error of about 2%, these are comparably large, almost equal and have to be subtracted. However, since h turns out to be the least critical dimension in this case, the tolerance estimate should be still sufficient for practical purposes.

		g		w		h	
		TE	TM	TE	TM	TE	TM
$\partial_q\beta/\mu\mathrm{m}^{-2}$							
(s)	FD	-0.280	-0.565	0.538	0.284	1.738	2.427
	PT	-0.335	-0.636	0.622	0.293	1.768	2.455
(a)	FD	0.075	0.201	0.645	0.475	1.820	2.602
	PT	0.075	0.199	0.737	0.489	1.850	2.559
$\Delta q/\mathrm{nm}$							
$L = L_c$	NUM	6.4	6.6	22	30	27	50
	PT	6.0	7.0	21	30	30	34
$L = L_c/2$	NUM	1.4	1.6	4.6	6.3	5.9	11.2
	PT	1.2	1.4	4.3	6.0	6.0	6.7

Table 1: Top: Gradients $\partial_q\beta$ of supermode propagation constants for TE and TM polarization and for modes of even (s) and odd (a) symmetry. Modified parameters are the spacing g, the width w, and the height h of the ribs. Values in rows 'FD' are calculated as difference quotients from two mode analysis runs on neighboured parameter values. Lines 'PT' contain the results of applying Eqs. (11, 12, 14, 15).
Bottom: Geometry tolerances Δq admissible for a power transmission deviation ΔP less than 1% for device lengths of L_c and $L_c/2$. 'NUM' indicates the limits read from the marker lines of Fig. 7, with the smaller difference taken in case of a nonsymmetric curve $P(\delta q)$. 'PT' refers to the results of the perturbational formulas and Eqs. (17, 18).
Parameters are identical to Fig. 6.

In a realistic device, input and output ports will not be formed by abrupt ending of the waveguides, but by diverging coupler arms, and then the above assumptions are certainly not admissible to calculate the exact power transmission. However, in this paper we have been interested in estimations for the fabrication tolerances only, and the main influence of a varied dimension on the output power should still arise from the supermode wavenumber shift, even in a more complex geometry. Therefore our analysis can be expected to yield reasonable estimates for devices including coupler arms and tapering as well. Maybe L must be substituted by an intermediate length between the actual length of the region with parallel waveguides and a dimension, outside of which the waveguides can be regarded as well separated.

4 Conclusions

Based on a single mode analysis, propagation constant gradients with respect to alteration of geometry dimensions can be estimated by the evaluation of line integrals along the relevant dielectric interfaces. We suspect the deviations between the perturbational gradients and the reference values, which were obtained as difference quotients from multiple mode calculations, to be blamed partly to the approximations entering formulas (9 - 15) and partly to the remaining inaccuracies in the numerically determined mode fields. Comparisons like that in Sec. 3.1 should indeed provide a good test not only for the perturbation formulas, but for the accuracy of the underlying mode solver.

However, the accuracy actually achieved in this study is sufficient to yield reasonable tolerance estimates for

our simple two waveguide coupler. Note that one mode analysis run (calculation of all supermode profiles and propagation constants) is required only, even for a more complex device defined by N dimensional parameters, where at least $N + 1$ simulations are necessary to evaluate the wavenumber gradients in a conventional way by difference quotients.

For given wavelength, a rectangular step index waveguide is prescribed by the waveguide dimensions and the refreactive index values. With the perturbation formulas considered in this paper and analogous expressions for small uniform refractive index perturbations, as emerge directly from Eq. (5) [1], derivatives of the propagation constants with respect to all relevant parameters are at hand. Regarding the automated optimization of a device geometry, these formulas give direct access at least to estimates for the partial derivatives of the objective function, the output power, at almost no extra cost. This should reduce the computational effort significantly in cases where one simulation is expensive already.

Guidelines for geometry tolerant directional couplers can be directly read off from Eqs. (17, 18) combined with the perturbational expressions. The total length should be kept short, intensities on dielectric boundaries must be low, and only modes with almost equal squared profiles should interfere. With relations for the power transfer analogous to (16), similar rules should be applicable to other devices based on multimode interference. Unfortunately, this usually conflicts with the desired device performance.

Acknowledgment

Financial support by Deutsche Forschungsgemeinschaft (Sonderforschungsbereich 225) is gratefully acknowledged.

References

[1] C. Vassallo. *Optical Waveguide Concepts*. Elsevier, Amsterdam, 1991.

[2] A. W. Snyder and J. D. Love. *Optical Waveguide Theory*. Chapman and Hall, London, New York, 1983.

[3] M. S. Stern. Semivectorial polarised finite difference method for optical waveguides with arbitrary index profiles. *IEE Proceedings, Pt. J*, 135(1):56–63, 1988.

[4] M. Wallenhorst, M. Niemöller, H. Dötsch, P. Hertel, R. Gerhardt, and B. Gather. Enhancement of the nonreciprocal magneto-optic effect of TM modes using iron garnet double layers with opposite Faraday rotation. *Journal of Applied Physics*, 77(7):2902–2905, 1995.

[5] M. Lohmeyer. Wave-matching method for mode analysis of dielectric waveguides. *Optical and Quantum Electronics*, 29:907–922, 1997.

[6] M. Lohmeyer. Vectorial wave-matching mode analysis of integrated optical waveguides. *Optical and Quantum Electronics*, 30:385–396, 1998.